Fabrication of Electroluminescent Carbon Fiber Composite for Damage Visualization

J. Qiu[1], M.K. Idris[2], G. Grau[2], G.W. Melenka [1]*
[1]Mechanical Engineering, York University, Toronto, Canada
[2]Electrical Engineering and Computer Science, York University, Toronto, Canada
* Corresponding author(gmelenka@yorku.ca)

Abstract

Conventional damage inspection methods and characterization of carbon fiber (CF) composites are typically destructive, expensive, and do not provide spatial resolution. Non-destructive monitoring of carbon fiber composites is presented with an electroluminescent (EL) thin-film dielectric phosphor sandwiched between compacted and semi-transparent dispersed CF composite lamina. Different fractural states in the CF composite cause EL luminance changes which allows for damage detection and localization in the CF through visual inspection. The proposed methodology offers simple and effective structural health monitoring to any product manufactured from CF ranging from aerospace to high-performance sporting goods.

Keywords: Structural Health Monitoring, Carbon Fiber Reinforced Polymer, Electroluminescence

1. Introduction

Carbon fiber (CF) composites have been adopted in application ranging from aerospace to energy due to their high strength to weight ratio, chemical resistance, as well as both thermal and electrical conductivity.[1] Textile Carbon Fiber Reinforced Polymer (CFRP) is a common CF composite that relies on interwoven CF yarns to provide strength and stiffness while a polymer matrix consolidates the structure for toughness and reinforces radial strength.[2] However, due to the complex fractural and failure mechanics of textile CFRP, it is difficult to measure and quantify damage in its lifecycle.[3] Structural Health Monitoring (SHM) is becoming increasingly common for composite structures as it avoids periodic inspections and provides permanent structural surveillance.[4] SHM sensing methods can be categorized into external and integrated. Conventional structural inspection relies on non-destructive testing (NDT) methods such as acoustic emission, eddy current or Bragg Grating, thermograph, and X-ray.[5] However, these methods rely on complex and costly equipment. In contrast, integrated SHM implements damage detection and characterization by embedding sensors within the structure or using the structure itself as the sensor. A novel method is proposed here utilizing electroluminescence (EL) to visualize damage for detection and characterization. Intrinsic electroluminescence (EL) is an electro-optic phenomenon in which a doped phosphor material emits light in response to a strong electric field, typically AC.[6] Traditionally, EL has been wildly adapted for lighting applications; however, here it is demonstrated that structural status can be visualized by EL luminance differences. In this work, a novel SHM manufacturing methodology for textile CFRP structures is presented

2. Methodology

2.1 Design Overview

An example of a conventional EL device structure and the proposed SHM EL structure is shown in Figure 1. The device structure utilizes two CF electrodes with a phosphor layer sandwiched between and is shown in Figure 1 (b).In this study, the integrated SHM sensing method of electrical impedance tomography (EIT) is taken a step further to visualize the non-visible internal damage of the CFRP in the form of electroluminescence (EL) variations induced by changes in electrical characteristics. [7]

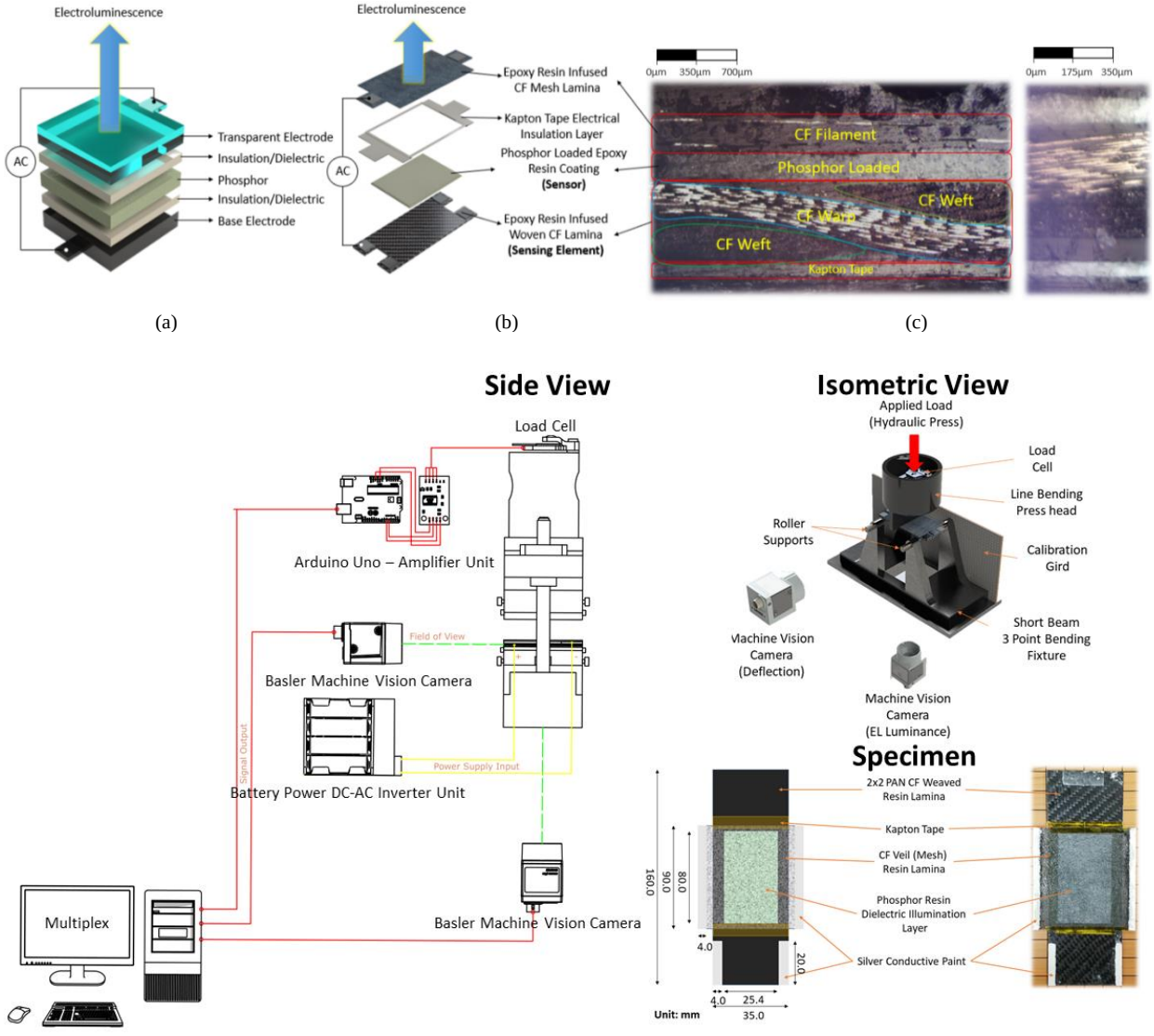

Figure 1 Comparison and modification between (a) Conventional EL structure and (b) SHM EL CFRP structure along with (c) 10x (left) and 40x (right) magnification cross-sectional microscopy of the structure. The mechanical flexural testing apparatus and standardized specimen are shown in (d).

The CFRP EL structure consists of three main layers. The sensing back electrode is a conventional epoxy resin infused woven CF lamina. The dielectric illuminating layer is epoxy resin loaded with dispersed phosphor powder. This is the sensor module displaying the

structural status of the woven CF lamina. The semi-transparent top electrode includes an epoxy resin infused CF veil lamina that allows light to escape for visualization. The overall structure is encapsulated with epoxy resin to contain the entire structure. This design utilizes the electrical conductivity of CF electrodes, the capacitive nature of an intrinsic EL device, and the visible light transmittance of the CF veil to develop the SHM device. Each component is identified in the cross-sectional microscopy of the composite structure shown in Figure 1(c). Conventional 3 point flexural bending test specimen standard stated by ASTM D2344 has been adapted as reference for standardize testing specimen with slight modification. To reduce specimen variation, dimension is standardized shown in Figure 1 (d).

2.2 Bottom Sensing Electrode: Epoxy Resin Infused Woven CF Fabric Lamina

The bottom sensing electrode is constructed by compression mold curing a woven CF fabric (two by two,0/90/0, 3k bundle, PAN carbon fiber) saturated in epoxy resin (2020/2000 system epoxy resin, Fibre Glast) at room temperature. The epoxy resin is applied to the woven CF fabric using a roller pressing to ensure saturation. Mold release (700-NC, Frekote) is applied to two smooth stainless-steel plates (3.5" x 15", US32D, Satin Stainless-Steel Plates, Rockwood) prior to compression curing the lamina with a manual hydraulic press (10-Ton hydraulic press, MAXIMUM). The resin surface and woven CF fabric roughness can be controlled by the curing pressure to manipulate electrical characteristics and optimize EL light output. These parameters are varied individually while keeping others constant to identify both structural and electrical characteristics of the CF fabric lamina and its corresponding EL luminance response.

2.3 Luminescent Dielectric: Phosphor Powder Loaded Epoxy Resin Dielectric

The thin-film dielectric phosphor coating is fabricated by blade coating epoxy resin precursor (2060/2000 system epoxy resin, Fib Glast) loaded with ZnS: Cu powder (29 μm Particle Size, Shanghai Keyan Phosphor Technology CO., LTD) on the bottom sensing electrode. The phosphor-loaded precursor is cured at room temperature until solidification. The lateral dimensions of the desired coating area are controlled by applying Kapton tape masking, while thickness is varied by applying multiple tape layers. The phosphor loaded resin precursor is semi-cured at room temperature for 3 hours prior to blade coating to prevent precursor reflow. Spin coating was used as a test process to characterize the effect of film thickness on electrical and structural characteristics and the corresponding EL luminance output. Dielectric constant and thickness are quantified by capacitance measurement with a parameter analyzer (4200A, Keithley) and stylus profilometry (Alpha-Step D-600, CN Tech) respectively. To adapt for mass manufacturing and industrial application, we replace spin coating to deposit the thin film phosphor layer with blade coating. Unlike spin coating, blade coating is a scalable method that should scale up to industrial dimensions.

2.4 Semi-Transparent Top Electrode: Epoxy Resin Infused CF Mesh Lamina

The semi-transparent top electrode fabrication process is coupled with the assembly and encapsulation process. CF veil (10g x 35.5", PAN, Composite Canada Fabric) is overlaid on top the cured phosphor loaded epoxy resin dielectric and secured with electrically insulating

Kapton tape (1” x 36 yds, 1 Mil, ULINE) on the boundary. The assembled structure is encapsulated by dip coating in epoxy resin (2060/2000 system epoxy resin, Fibre Glast) and heat cured in an isothermal oven at 90 ˚C for 30 minutes.

2.5 Data Acquisition and Processing

The flexural failure mode of the structure is investigated through a 3-point bending apparatus consisting of an adjustable flexural fixture and an upper anvil made from polylactic acid (PLA) coupled with an Arduino-controlled load cell referencing the ASTM D2344 standard.[8] The specimen is illuminated with a 108V-6kHz power source. A machine vision camera (acA2440-35µm, Basler) with a 50mm focal length lens (MVL50M23, Navitar) captures the EL response during both characterization and flexural testing. A second machine vision camera captures the deflection to record the stress-strain relation. Acquisition and processing are automated using MATLAB to acquire loading, deflection, and EL response simultaneously to produce numerical relations between these variables.

3. Results and Discussion

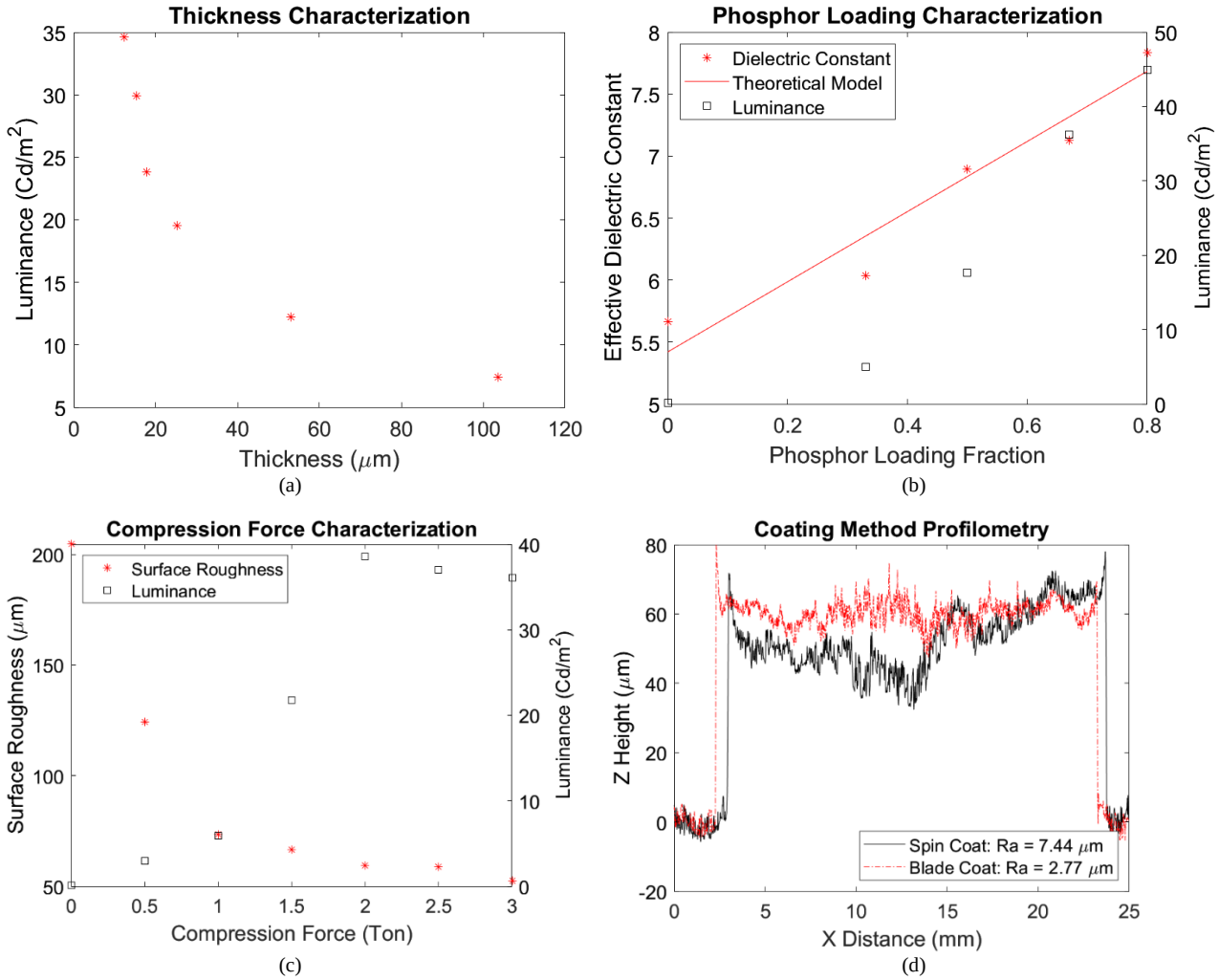

Figure 2 EL response is characterized as a function of fabrication parameters of the epoxy resin infused woven CF fabric lamina and phosphor loaded epoxy resin coating: (a) dielectric thickness, (b) phosphor loading fraction, and (c) woven CF lamina compression force. Dielectric constant in (b) follows linear trend with phosphor loading fraction as expected from theoretical model. (d) Profilometry of phosphor loaded epoxy resin coating shows obvious improvement in thickness variation from spin coating to blade coating.

3.1 Characterization

The fundamental purpose of fabrication parameter characterization is to determine the fabrication settings for optimal visualization conditions in terms of brightness and contrast. In terms of damage inspection techniques, the resolution of image acquisition depends greatly on the EL luminance output of the specimen. Image quality of the inspection method directly impacts the localization and identification of the damage state on the specimen. The goal of optimizing different processing parameters is therefore to maximize luminance and hence enhance damage detection. Visualization of the EL on the CFRP structure can be characterized in terms of EL luminance magnitude and patterns. As shown in Figure 2 (a), (b) and Figure 3 (a), (b), EL luminance is proportional to phosphor loading fraction and the inverse of coating thickness. However, phosphor powder serves not only as the illuminating center, but also as the dielectric. In Figure 2 (b), the experimental dielectric constant of phosphor loaded epoxy resin is shown as a function of phosphor loading fraction [9]. EL luminance is found to be directly proportional to the capacitance of the structure, i.e. proportional to the inverse of dielectric thickness and proportional to dielectric constant. The EL illumination pattern can be classified as woven CF fabric, CF mesh, or a mix of both depending on the compression force applied to the lamina during the curing process. Shown in Figure 2 (c), EL illumination cannot be observed if no compression mold is used due to the large thickness of the epoxy layer on the CF weave and large surface roughness of the resulting lamina (202μm).With sufficient pressure, a uniform lamina base is formed with decreasing roughness and increasing EL luminance as compression pressure is increased. The transition of EL patterns from CF mesh to woven fabric can be clearly observed with increasing compression force (see Figure 3 (c)). With higher phosphor loading, specimens present higher peak EL luminance shown in Figure 3 (b). Specimens produced by spin coating exhibit thickness variations inherent to spin coating of high-viscosity fluids with particle loading. The thickness is increased at the center leading to decreased luminance, which is especially obvious for thick coatings as indicated in Figure 3(a). Shown in Figure 2 (d), blade coating is more controllable achieving uniform thickness (Ra = 2.77μm) irrespective of phosphor loading and is suitable for large-scale manufacturing. Overall, 70% phosphor loading, 4-ton compression force, and 34.7-μm coating thickness demonstrate the optimal EL visualization result without dielectric breakdown with 108V-6kHz power supply.

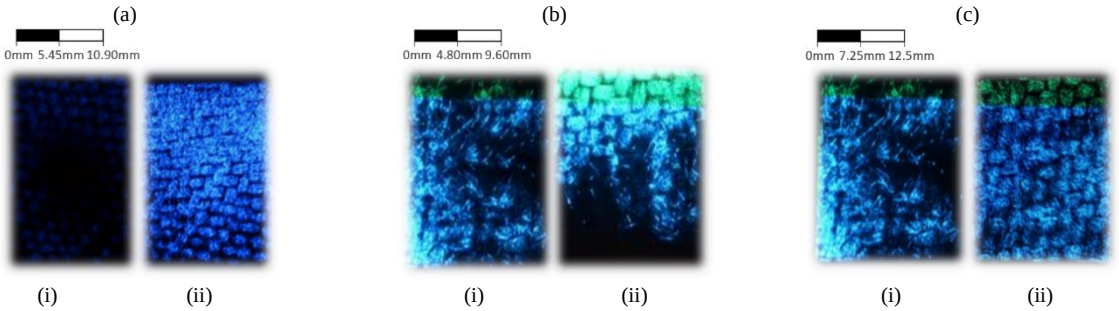

Figure 3 Photographs showing El luminance pattern for different processing conditions. (a) Devices with thin phosphor resin (7µm) (ii) exhibit strong EL luminance compared to (i) thick coating (220 µm). (b) (i) Low phosphor loading (0.5) shows only minimal light output and (ii) high phosphor loading increases the peak luminance output. One can also observe reduced brightness at the center due to the non-ideality of the spin coating process. (c) (i) For low compression force (below 1 ton), the mesh pattern of the CF veil top electrode dominates. (ii) For high compression force (above 2 ton), the weave pattern of the woven CF bottom electrode dominates.

3.2 Damage Sensing

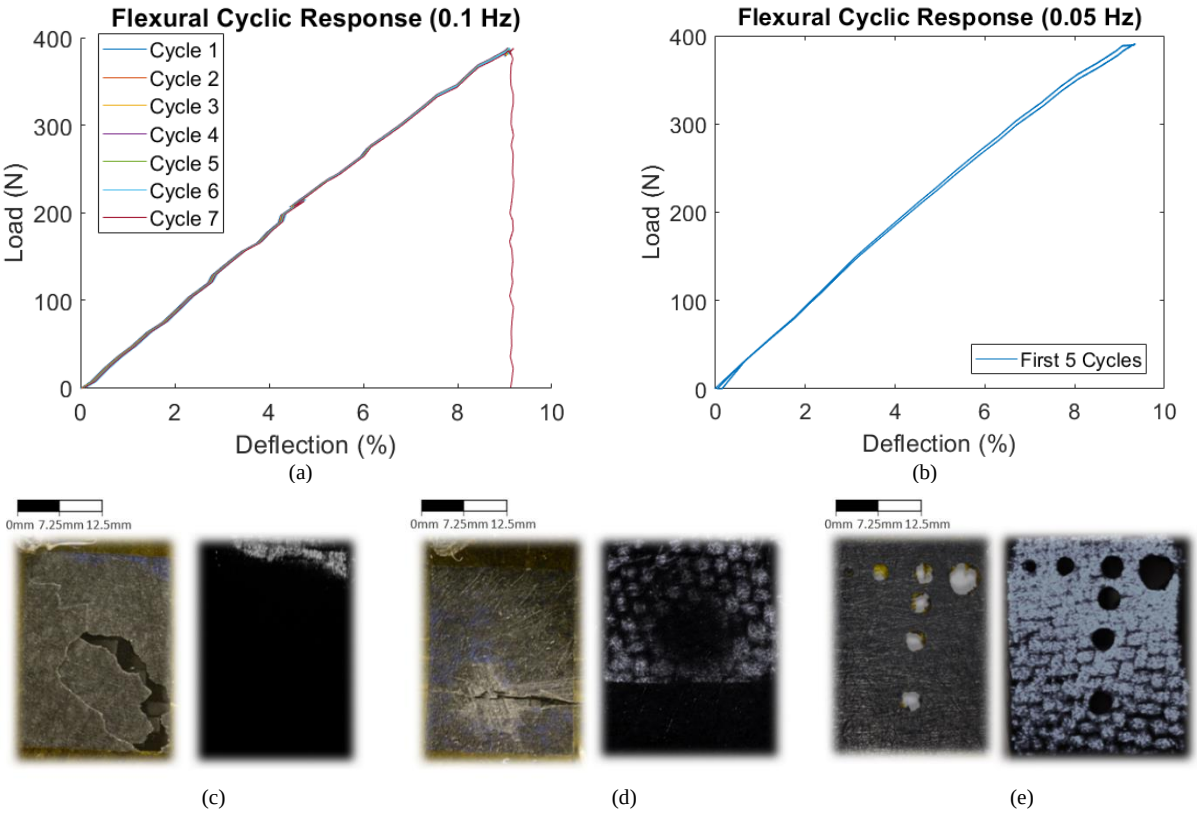

Figure 4 Mechanical Flexural Testing of Standardized Specimen Response in: (a) 0.1Hz and (b) 0.05 Hz. Damage visualization by EL response: (b) Debonding, (c) Crack, (d) Puncture. Left: Photo of damage without applied voltage. Right: With applied voltage, the structure lights up and damaged regions can be clearly identified as dark areas.

Debonding, fracture, and puncture have been selected to demonstrate the failure mode inspection. Fatigue analysis in the form of flexural cyclic loading is utilized to simulate the lifecycle of the device. As illustrated in Figure 1(d) above, the load and deflection of the 3 point flexural fatigue mechanical test are acquired by embedded load cell and machine vision camera respectively. An FDM printed press head is supplying line load to the specimen under roller support condition. Flexural fatigue induced damage is characterized with image

acquisition at two different frequency setting: 0.1 Hz (High) and 0.05 Hz (Low) shown in Figure 4 (a) (b)to categorized debonding and matrix cracking damage respectively. Throughout the experiments with a series of specimens, debonding and matrix cracking were consistently identified as failure modes. In the lifecycle of the sensing device, debonding and crack are likely to occur. Debonding or detachment of layers are bound to occur due to the weak adhesion between dissimilar materials. [10] In Figure 4 (c), low frequency cyclic loading causes matrix (phosphor layer) cracking and detaching of the EL phosphor sensor layer. However, no damage can be observed in the CFRP sensing layer, this is a clear indication of debonding. With high frequency fatigue test, the entire specimen displays clean fiber fracture without presence of delamination or debonding shown in Figure 4 (d). Specifically, the illumination at upper section of the specimen remains. Structurally, the load bearing capacity of the sensor sandwich layer (phosphor loaded resin) is substantially lower than the CFRP layer. Additionally, realistic application will typically utilize more than one CFRP layer. Therefore, the structural response of the entire device is dominated by the CFRP layer(s). The sole purpose of the sensor layer is to operate prior to fiber fracture. Once the sensor layer has failed, it is a clear indication of matrix failure. Beyond this point, the composite material would not be considered as structurally stable or reliable.

For the purpose of evaluating the sensitivity and resolution, circular punctures are made at various diameter and separation distance (see Figure 4 (d)). This is an attempt to determine detection limit at which the dimension and location of damage can still be identified. The smallest circular damage of diameter 1/16” (top left) is barely visible without EL illumination but can be clearly identify once illumination is active. This highlights the benefits of the EL layer for amplifying damage inspection.

4. Summary and Outlook

SHM and damage visualization utilizing a novel EL CFRP are demonstrated. The proposed fabrication process is compatible with traditional CF composites and can detect damage. The fabrication parameters were optimized to maximize luminescent output and damage visualization. Damage in the CF structure due to bending can be clearly observed as variations in EL luminance. Mechanical flexural, tensile, and fatigue tests will be utilized next to investigate different failure modes and their effect on the EL luminance variations. The damage type will be characterized through the EL response. The process described in this work will also be scaled up for larger scale sensing and illumination.

5. Acknowledgement

We acknowledge funding support from York University through the Lassonde Innovation Fund (LIF), Dr. James Wu Research Internship and the Research at York (RAY) program. We acknowledge equipment use at the York University Electrical and Mechanical Engineering shared fabrication and characterization facilities and technical support from the technicians.

6. References

[1] B. A. Newcomb, “Composites : Part A Processing , structure , and properties of carbon fibers,” *Compos. Part A*, vol. 91, pp. 262–282, 2016.

[2] Bilisik K, “Characterizing the deformation of woven textile composites,” *SPE Plast. Res. Online*, no. September, pp. 1–3, 2017.

[3] Q. Sun *et al.*, “Failure criteria of unidirectional carbon fi ber reinforced polymer composites informed by a computational micromechanics model,” *Compos. Sci. Technol.*, vol. 172, no. December 2018, pp. 81–95, 2019.

[4] J. Cai, L. Qiu, S. Yuan, L. Shi, P. Liu, and D. Liang, “Structural Health Monitoring for Composite Materials,” *Compos. Their Appl.*, no. August, pp. 36–60, 2012.

[5] Y. K. Zhu, G. Y. Tian, R. S. Lu, and H. Zhang, “A review of optical NDT technologies,” *Sensors*, vol. 11, no. 8, pp. 7773–7798, 2011.

[6] G. Liang *et al.*, “Coaxial-Structured Weavable and Wearable Electroluminescent Fibers,” *Adv. Electron. Mater.*, vol. 3, no. 12, pp. 1–10, 2017.

[7] Z. H. Xia and W. A. Curtin, “Damage detection via electrical resistance in CFRP composites under cyclic loading,” *Compos. Sci. Technol.*, vol. 68, no. 12, pp. 2526–2534, 2008.

[8] T. Laminates, “ASTM D2344 for Short beam Strength.pdf,” vol. 03, 2000.

[9] N. A. Bani, H. Ahmad, F. Muhammad-sukki, and A. Abubakar, “Modelling of Electroluminescence in Polymeric Material using Dimensional Analysis Method : Effect of Applied Voltage and Frequency,” no. April, 2015.

[10] S. Feldfogel and O. Rabinovitch, “International Journal of Solids and Structures Two dimensional dynamic debonding in FRP strengthened plates,” vol. 170, pp. 95–110, 2019.